2014 IEEE International Conference on Robotics & Automation (ICRA)
Hong Kong Convention and Exhibition Center
May 31 - June 7, 2014. Hong Kong, China

Lower Body Exoskeleton-Supported Compliant Bipedal Walking for Paraplegics: How to Reduce Upper Body Effort?

Barkan Ugurlu[1], Hironori Oshima[2], and Tatsuo Narikiyo[2]

Abstract— **This paper introduces a position-based compliance control algorithm that can be implemented in a lower extremity exoskeleton-supported paraplegia walking task, in which upper body has to be utilized to maintain the overall balance. In order to reduce the upper body effort required during the task, the controller is designated to be capable of managing the position/force trade-off in conjunction with an active admittance regulator scheme. In the case of no force errors, the controller prioritizes position tracking in a way to achieve walking support. Once the force error increases (e.g., ground reaction force peaks, unexpected disturbances, stepping on an object, etc.) the position reference is updated in accordance with the force constraints and active admittance characteristics. By the virtue of this strategy, the human-robot system exhibits enhanced environmental interaction capabilities; therefore, the subject can maintain the overall balance with relatively less upper body effort while walking. Implementing the proposed method, we conducted robot-assisted walking experiments on 4 able-bodied subjects with different body mass index levels and genders. Subjects were instructed to be in passive mode. In addition, walking with severe obstacles was also experimented on a single able-bodied subject. In conclusion, the proposed method enabled us to yield enhanced walking performance comparing to classical rigid position control scheme; indicating that it could potentially introduce a compliant locomotion control alternative for the paraplegia walking support task with a comparatively less amount of upper body effort requirements.**

I. Introduction

Comparing to their wheeled counterparts, robotic lower body exoskeletons possess clear advantages in improving the health and life quality of non-ambulatory patients [1]. Individuals with wheeled assistive equipment are reported to be prone to pressure sores and related diseases [2]. Furthermore, such devices may not provide an overall ambulatory support within the presence of uneven surfaces and narrow pathways.

In response to this matter, engineers from Ekso Bionics (http://www.eksobionics.com) presented eLegs, which was developed as an end-result of Kazerooni's contributions [3]. Following a similar trend, researchers introduced ReWalk, an electrically-actuated lower body exoskeleton with clinically demonstrated assistive capabilities [4]. In another examples, Kagawa and Uno proposed WPAL, a gait assist device that can be single-handedly worn from a wheelchair [5]. Sankai et al. engineered HAL, an intention-driven exoskeleton [6]. Most of these devices are experimented on individuals with no inherent walking ability and they utilize the human-wearer's upper body motion via auxiliary tools, e.g., canes.

Above-mentioned devices appear to be successful attempts for the paraplegia support and they are in the process of commercial development. Considering the target task, they naturally rely on stiff position tracking schemes. While remarkably useful in its own right, this approach may not provide a satisfactory and comfortable walking experience; the human-wearer may face difficulties while the exoskeleton system has noncompliant contact with the ground, e.g., touch-down of a swing leg or stepping on an uneven object. Therefore, it is anticipated that a compliant exoskeleton may provide a relatively more feasible support for a wearer.

Addressing these issues, Caldwell et al. underlined the importance of compliance in their design and control procedures [7]. Veneman et al. introduced LOPES, an impedance-controlled exoskeleton [8]. Neuhaus et al. built an exoskeleton system, called Mina, powered via electrical actuators that can be compliantly driven with a position/force control strategy [9]; however, in-depth discussions regarding the compliance control are not disclosed.

In the light of these contributions, we built an electrically-actuated and actively-compliant whole body exoskeleton prototype, named TTI-Exo, which shares the common ground with [7]–[9], in terms of control philosophy. In our approach, the motion generator firstly synthesizes target position references in a physically-viable manner. Ground reaction force references are also generated in accordance with the target motion references. Utilizing the force measurements and force references, the controller then generates joint displacements that correspond to force error, via Jacobi transpose and virtual admittance blocks. In addition to position constraints, these joint displacements are fed-back to local servos, so that the position/force trade-off is managed in a compliant manner. As the result, exoskeleton-based paraplegia support task can potentially be achieved more comfortably for the wearer; he/she needs to exert comparatively less upper body effort to maintain the overall balance while the human-robot system is interacting with the environment.

The contributions of this paper can be categorized in two fractions: i) An actively-compliant locomotion control algorithm is proposed for the exoskeleton-based paraplegia walking support task. The controller introduces the position/force trade-off management in a compliant manner, and therefore, hypothetically outperforms classical stiff position control strategy in terms of reduced upper body effort. To the authors' knowledge, this paper reports one of the first

[1]B. Ugurlu is with the Department of Brain Robot Interface, Computational Neuroscience Laboratories, Advanced Telecommunications Research Institute International (ATR), 2-2-2 Hikaridai, 619-0288 Kyoto, Japan. e-mail: barkanu@ieee.org

[2]H. Oshima and T. Narikiyo are with the Department of Advanced Science and Technology, Control Systems Laboratory, Toyota Technological Institute (TTI), 2-12-1 Hisakata, Tempaku, 468-8511 Nagoya, Japan. e-mail: n-tatsuo@toyota-ti.ac.jp

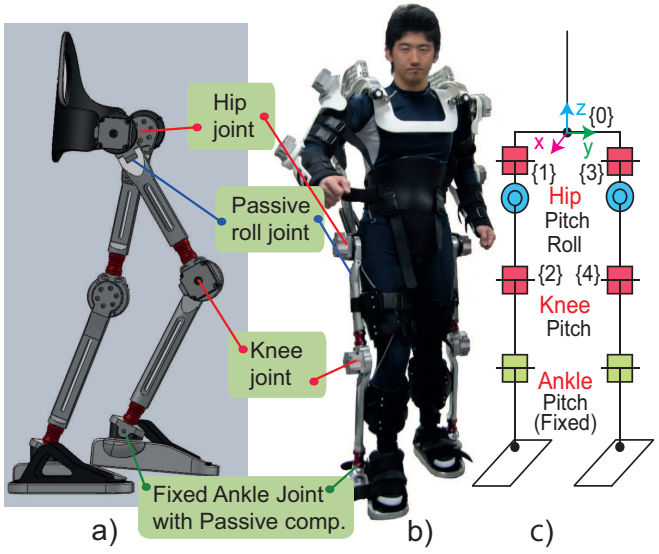

Fig. 1. a) Lower body CAD model of TTI-Exo. b) TTI-Exo, being worn by an able-bodied subject. c) Joint configurations; Active DoF: red, passive DoF: blue, fixed DoF with flexible but firm enough material: green.

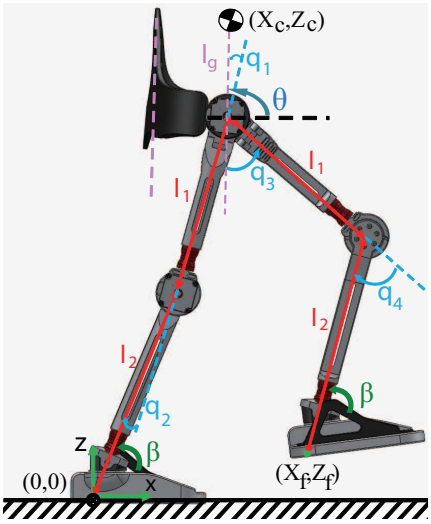

Fig. 2. Kinematic parameters on the CAD model. CoM is assumed to be l_g meters above the hip. Link lengths (l_1, l_2, l_g) are adjusted for each wearer. θ denotes pitch orientation, q_i are active joint angles ($i = 1, 2, 3, 4$). Ankle angle is fixed to β degrees with the help of a stiff-enough flexible material, so that the stride length can be extended ($\beta < 90^o$).

attempts to address upper body effort minimization for the exoskeleton-supported paraplegia walking task. In relation to this matter, we define performance criteria based on upper body motions for a quantitative evaluation. ii) In addition to flat surface walking trials, this paper experimentally evaluates exoskeleton-based walking support within the presence of severe obstacles, a crucial case which was not heavily investigated in the literature.

It should be noted that TTI-Exo is in a less mature phase, by means of clinical applicability, comparing to the existing systems. The central idea is to build a prototype, investigate the issues that are not heavily mentioned in the literature, and convey information to the next phase. Therefore, this paper appears to be a step towards exoskeleton-based paraplegia walking support, and thus, clinical experiments are addressed as future studies.

This paper is organized as follows. In section II, we briefly introduce the mechatronics hardware of TTI-Exo. Motion generation and control algorithms are disclosed in sections III and IV, with sufficient details. Experimental results are thoroughly discussed in section V, and finally, the paper is concluded in section VI.

II. Lower Extremity Exoskeleton: TTI-Exo

In order to investigate the principles of robot-assisted paraplegia walking support, we built an electrically-actuated whole-body exoskeleton, named TTI-Exo. Its upper body is previously utilized for upper body rehabilitation and power augmentation tasks [10]. Fig. 1 displays the actual system with an able-bodied wearer, its CAD model and joint configurations.

Each leg is powered via 2 electrically-actuated active DoF (degrees of freedom), in hip and knee joints. Therefore, the robot has no inherent balancing ability; the wearer is expected to counterpose for the equilibrium via his/her upper body. Such an approach is previously proved to be viable for the task [3]–[5], [9]. What is more, using less number of actuators may help us to contain costs, so that these systems can be promoted in a larger scale. TTI-Exo is also equipped with passive hip joints about roll axis to allow lateral leg movements. Ankle joints are fixed with a flexible but firm enough material to reduce touch-down impacts. The system is attached to the wearer using straps and C-shaped braces. Link lengths are also adjustable for different wearers in a way to align robot and human joints. On this matter, potential hyperstaticity issues will be covered in our future work [11].

In its sensory system, 4 force sensing units are placed under each feet sole to measure vertical GRF (Ground Reaction Force), F_z, and horizontal CoP (Center of Pressure), X_{cop}. In addition, using F_z and X_{cop}, horizontal GRF, F_x, can be estimated as well.

$$F_z = \sum_{i=1}^{n} f_i; \;\; X_{cop} = \frac{\sum_{i=1}^{n} (f_i \; r_{ix})}{F_z}; \;\; F_x = \frac{X_c - X_{cop}}{Z_c} F_z \qquad (1)$$

In (1), f_i and r_{ix} are the i^{th} force sensor output and i^{th} force sensor position in x-axis, with respect to the related foot sole center. X_c and Z_c stands for the actual CoM position and can be computed via forward kinematics. n is the number of force sensors; $n = 4$ for each foot.

III. Motion Generation

A. Swing Foot and CoM Motion References

For the motion generation task, researchers usually make use of healthy human walking data [9]. In order to simplify

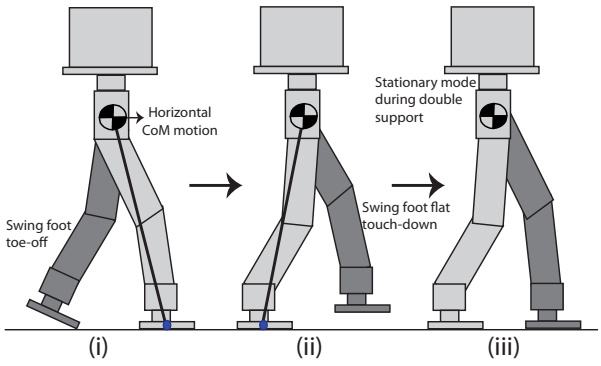

Fig. 3. During single support phases, the support foot center is chosen as the origin. During double support phases, both feet and CoM are stationary; these phases appear to be delay periods between sequential single support phases, for the purpose of maintaining the balance with less effort. Ankle angle is normally less than 90^o, but shown as 90^o for illustrative purposes.

this task, x-axis CoM position (X_c), upper body pitch orientation (θ), x-axis and z-axis foot trajectories (X_f, Z_f) are synthesized via polynomial interpolation, in a way to create smooth and continuous time-varying trajectories. These particular 4 inputs are determined to be convenient in our 4-DoF system for the paraplegia walking support task. Boundary conditions are carefully set by considering the desired stride length, mean target forward velocity, single/double support time periods. Likewise, X_f and Z_f trajectories are generated to have zero velocity and acceleration at the moment of touch-down to reduce possible impacts. The motion generator makes sure that single/double support phases are tied seamlessly, so that trajectories are always continuous both in position, velocity and acceleration levels. It is also possible to alter motion generation parameters (stride length, mean forward velocity, single/double support time periods) in real-time, so as to make sure the human subject comfortably receives walking support.

Since only static equilibrium is considered, it is the human-wearer upper body motion that guarantees the overall dynamic balance is maintained, in a similar manner as performed in [3]–[5], [9]. Due to the inherent underactuation in TTI-Exo, CoM height (Z_c) and swing foot orientation could not be imposed as inputs in our motion generator. Instead, (X_c, θ, X_f, Z_f) are analyzed to be relatively significant and selected as inputs for our 4-DoF system. They are indicated on the CAD model in Fig. 2. Moreover, motion generation parameters are carefully selected and trajectories are double-confirmed in kinematics simulations, so as to keep CoM height within a small range and make sure the swing foot leaves the ground with toe-off, then touches down with a flat orientation to avoid possible impacts (see Fig. 3).

GRF references are computed as below, where m is the overall mass (the wearer+exoskeleton), g is the gravitational acceleration. ref underscript refers to referential values; 1 and 2 additions in the underscripts respectively associate the related parameters to left and right feet. Note that eqs. (2) and (3) are arranged for left foot single support phase and an identical approach can be followed for right foot single support phase. Equation (4) stands for double support phase.

$$F_{xref1} = m\ddot{X}_{cref};\ F_{zref1} = m(\ddot{Z}_{cref}+g); \quad (2)$$
$$F_{xref2} = 0;\ F_{zref2} = 0; \quad (3)$$
$$F_{xref1} = F_{xref2} = 0;\ F_{zref1} = F_{zref2} = 0.5mg. \quad (4)$$

Since x-axis CoM trajectory is polynomially generated during single support phases, $\ddot{X}_{cref}$ can be previously obtained for (2). Moreover, z-axis CoM is within a very small range, and thus, $\ddot{Z}_{cref}$ can be neglected. Swing foot force references are naturally set to zero (eq. (3)). During double support phases, there is no horizontal motion. Because of this reason, horizontal force references are set to zero. Vertical force references are half of the total weight for the both feet.

B. Joint Angle References

For a given set of referential x-axis CoM position (X_c), upper body orientation (θ) and swing foot position (X_f, Z_f) parameters, joint angles can be analytically computed via the following inverse kinematics algorithm.

$$c_2 = \frac{X_c - l_2\cos\beta - l_g\cos\theta}{l_1};\ s_2 = \pm\sqrt{1-c_2^2} \quad (5)$$
$$q_2 = \beta - atan2(s_2,\ c_2) \quad (6)$$
$$q_1 = \beta - \theta - q_2 \quad (7)$$
$$X_a = X_f - l_2\cos\beta - l_1\cos(\beta - q_2) \quad (8)$$
$$Z_a = Z_f + l_2\sin\beta + l_1\sin(\beta - q_2) \quad (9)$$
$$c_4 = \frac{X_a^2 + Z_a^2 - l_1^2 - l_2^2}{2l_1l_2};\ s_4 = \pm\sqrt{1-c_4^2} \quad (10)$$
$$q_4 = atan2(s_4,\ c_4) \quad (11)$$
$$h_1 = -l_1\cos\theta - l_2\cos(q_4+\theta) \quad (12)$$
$$h_2 = l_1\sin\theta + l_2\sin(q_4+\theta) \quad (13)$$
$$s_3 = \frac{h_2X_a + h_1Z_a}{h_1^2+h_2^2};\ c_3 = \pm\sqrt{1-s_3^2} \quad (14)$$
$$q_3 = atan2(s_3,\ c_3) \quad (15)$$

Sequential computation of (5)-(15) reveals all 4 joint angles, in which fixed ankle angle β is given beforehand. This solution is singularity free for all the configurations, except fully straightened knee angles. See Fig. 2 for the definition of kinematic parameters on the CAD model. Note that X_a, Z_a, h_1, h_2, c_2, s_2, c_4, s_4, c_3 and s_3 are intermediate parameters to ease the calculations.

IV. Compliant Motion Control

Fig. 4(a) encapsulates the implemented block diagram in a broad scope [12]. Fig. 4(b) provides a detailed look into the active compliance control block, named Virtual Admittance Controller (VAC). In these figures, τ_{cmd}, τ_{fr}, τ_{cg}, τ_{sv} refer to motor command torque, friction compensation torque, coriolis & centrifugal and gravity compensation torque, servo controller output torque, respectively. F and q stand for GRF and joint angles. Underscripts v, err and ref sequentially indicate the output of VAC, error and referential values, whereas measured values possess no underscript.

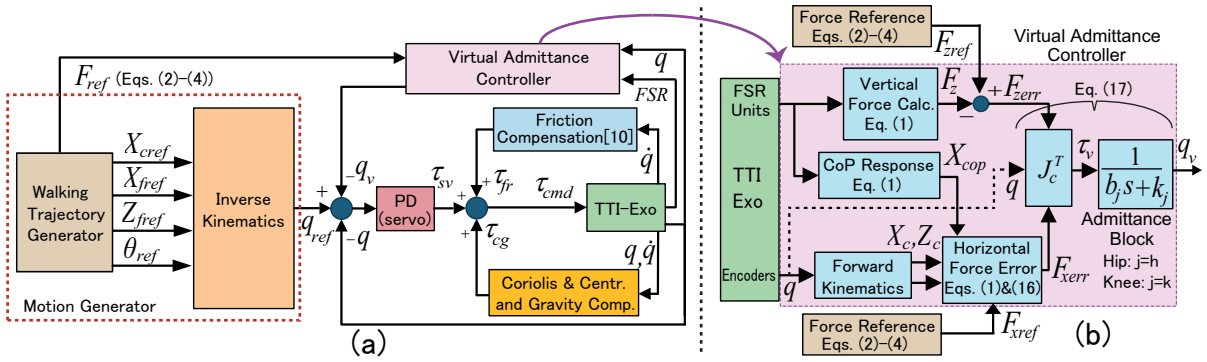

Fig. 4. a) The implemented block diagram in a broad scope. b) A closed look into the Virtual Admittance Controller (VAC) for a single leg.

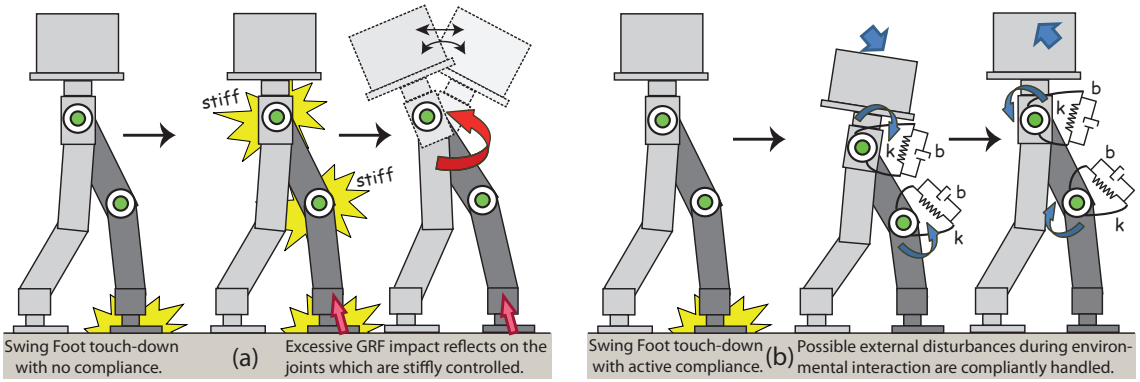

Fig. 5. a) With stiff joint tracking strategy, external forces, such as inevitable GRF impacts, directly reflect on the robot body. This may badly influence the overall dynamic balance; the impact may produce disturbances on the subject, and she/he may need to exert extra upper body effort to maintain the equilibrium. In that case, undesired torso angle fluctuations and horizontal movements could be experienced. b) With virtual admittance control strategy, possible external disturbances are handled compliantly. Within the presence of excessive forces, joint tracking is partially sacrificed and joint stiffness is decreased. As soon as the excessive force vanishes, the joint stiffness turns back to its initially-set value.

Motion generator includes Walking Trajectory Generator block and Inverse Kinematics block, which are explained in section II. In principle, it assesses timing profile (single/support periods), target mean forward velocity and desired stride lengths, and then produces feasible joint angle references (q_{ref}). It also synthesizes necessary force references (F_{ref}). These joint angle references are inserted to servo control blocks (PD), together with the VAC output (q_v), to drive the actuators. VAC output simply tells us how much we should update referential joint angles ($q_{ref} : q_{ref} - q_v$), in a way to comply with the force constraints. In addition, compensation schemes are added as feedforward terms to enhance the mechanical performance of the system.

A. Virtual Admittance Controller

Virtual Admittance Controller is the main controller unit and it is mainly responsible for a safe and compliant environmental interaction between the human-robot system and the environment. Fig. 4(b) illustrates its working principle in detail. Firstly, it computes the GRF errors, ($F_{xerr\mu}, F_{zerr\mu}$), occurred in each foot, depending on the phase information (single/double support). Additional μ letter in underscripts refers to the leg number; left: $\mu = 1$, right: $\mu = 2$.

$$F_{zerr\mu} = F_{zref\mu} - F_{z\mu}; \qquad F_{xerr\mu} = F_{xref\mu} - F_{x\mu}. \quad (16)$$

Recall that referential force values are computed as shown in (2)-(4), while measured values are obtained via (1). The joint displacement vector that correspond to GRF errors, $q_{v\mu}$, may be calculated as follows.

$$q_{v\mu} = \overbrace{\begin{bmatrix} \frac{1}{b_{h\mu}s+k_{h\mu}} & 0 \\ 0 & \frac{1}{b_{k\mu}s+k_{k\mu}} \end{bmatrix}}^{Y_v:\ Admittance\ Block} \left(J_{c\mu}^T \begin{bmatrix} F_{xerr\mu} \\ F_{zerr\mu} \end{bmatrix} \right) \quad (17)$$

In (17), $J_{c\mu}$ is the Jacobian matrix that is defined between the μ^{th} foot center and the CoM position. ($b_{h\mu}$, $k_{h\mu}$) and ($b_{k\mu}$, $k_{k\mu}$) couples denote virtual damper and spring coefficients, respectively associated with the μ^{th} leg's hip and knee joints. Y_v is a diagonal admittance matrix and s is Laplace variable.

Assessing Fig. 4(b), it is possible to see that joint position reference, q_{ref}, is updated for about q_v degrees in a way to comply with the force constraints. At this stage, one may think that directly feed-backing τ_v term (see Fig. 4(b)) could function in the same way. However, directly feed-backing

TABLE I

EXPERIMENT PARTICIPANTS' DATA

	Age	Height [m]	Weight [kg]	Gender
Subject #1	24	1.52	43+(exo:21)	Female
Subject #2	31	1.75	71+(exo:21)	Male
Subject #3	30	1.62	48+(exo:21)	Female
Subject #4	60	1.67	63+(exo:21)	Male

TABLE II

EXPERIMENT #1 RESULTS, PERCENTAGE DECREASES IN RMS

	Horizontal Acc.	Pitch Rate	Forces from Arms
Subject #1	38%	51%	41%
Subject #2	47%	58%	32%
Subject #3	46%	57%	40%
Subject #4	33%	44%	53%

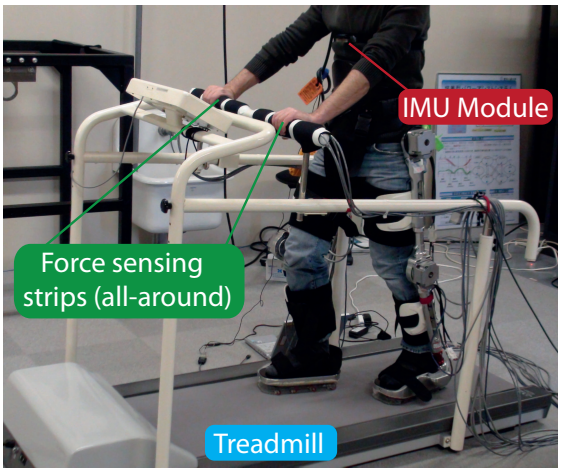

Fig. 6. Hardware setup during the experimentation period of Subject #2. IMU sensor is firmly attached to the wearer's chest to measure horizontal acceleration and pitch axis torso angle rate change variation. Treadmill handhold is covered with force sensing strips to measure the upper body force exerted by the wearer's arms. Refer to the multimedia attachment to view the experiments [13]. Note that force sensing units at the feet soles are not indicated in this figure.

τ_v does not necessarily associate active compliance with a force feedback strategy. In VAC method, both position and force constraints are simultaneously processed, so as to automatically manage the position/force trade-off via virtual admittance coefficients. For instance, if the force error suddenly gets bigger within the presence of a disturbance, VAC generates q_v term to decrease stiffness in a way to reduce force error. As soon as the disturbance vanishes, force error diminishes and q_v converges to zero. In that case, the joint turns back to its initial stiffness and continue strict joint position tracking. In other words, the joint gets softer if only force error appears; apart from this situation, it always keeps its initial stiffness for strict position control which is required for the task. The degree of *getting softer*, i.e., position/force trade-off, is software-controlled via virtual admittance coefficients. Fig. 5 illustrates both stiff position control and VAC strategies, in which touch-down impact is particularly examined.

B. Compensation Schemes: Friction, Coriolis and Gravity

In the proposed method, coriolis & centrifugal and gravity terms are computed via floating-base inverse dynamics and added as feedforward torques only for the robot side (not for the wearer). Furthermore, inherent joint friction hysteresis (stiction and viscous friction) model is previously identified, then corresponding friction compensation torque is also added as feedforward terms [10]. τ_{cg} and τ_{fr} in Fig. 4(a) refer to these terms. Partial dynamic compensation and friction compensation allow us to achieve position tracking with comparatively lower servo PD gains, so that the inherent joint stiffness could be reduced. This creates certain advantages in terms of human-robot interaction and enhanced mechanical performance.

V. EXPERIMENTAL RESULTS AND EVALUATIONS

In order to gain insights regarding the efficiency of Virtual Admittance Controller method over the conventional stiff position control strategy, we conduct robot-supported walking experiments with the help of 4 able-bodied volunteer subjects whose data are summarized in Table I. Experiments are conducted on a treadmill and the participants are instructed to be in passive mode. On this matter, we would like to highlight the fact that subjects can neither alter nor withstand the designated walking motion, as the exoskeleton is principally position controlled in both VAC and conventional methods.

Two types of experiments are executed: i) Experiment #1: Flat surface walking; ii) Experiment #2: Irregular surface walking. In order to perform a solid comparison, both Experiment #1 and Experiment #2 are executed twice; with the proposed VAC method and with the conventional position control method [3]–[5]. Refer to the multimedia attachment, to view various additional scenes from the experiments conducted with Subject #2 [13].

All experiments are conducted on a treadmill. Fig. 6 shows the hardware setup during the experimentation period of Subject #2. As illustrated in Fig. 5, conventional stiff position control scheme is unable to handle environmental interactions adroitly, such as touch-down impacts. Walking gaits that are controlled with the stiff control strategy is prone to undesired torso angle fluctuations and extra horizontal movements; making the wearer exert more and more effort to maintain the overall balance. Therefore, their arms may have to generate larger forces. On the other hand, the proposed VAC method overcomes this environmental interaction issue in a compliant manner; aforementioned undesired motions are observed in relatively fewer amounts.

To quantitatively corroborate our hypothesis, we collect horizontal acceleration and pitch angle rate change from each subjects' upper body via an IMU unit. Furthermore, treadmill handhold is covered with force sensing strips to measure the upper body force exerted by the wearer's arms. Acquired data are low pass filtered and trends are removed. All the processed data give us certain clues to quantitatively evaluate exoskeleton-based walking support performance. If the wearer exerts relatively less force from his/her arms,

and experiences less horizontal acceleration/pitch angle rate variations, we may categorize that case as a favorable case. Therefore, the proposed method, VAC, is compared with the conventionally used [3]–[5] stiff position control, by using the aforementioned upper body motion data.

Walking parameters are designated by considering the subject's leg lengths. For instance, single and double support time, forward velocity and stride length parameters are respectively designated as 1.2 [s], 0.12 [s], 0.7 [km/h] and 26 [cm] in the case of Subject #1. Having designated the walking parameters for a specific subject, she/he performed all the experiments with the same gait. In other words, gait remains the same in all the experiments for a given subject.

A. *Experiment #1: Flat Surface Walking*

In accordance with the above methodology, this experiment is conducted on 4 able-bodied subjects. Results on Subject #1 is depicted in Fig. 7. Solid purple and green lines symbolize variations, respectively associated with VAC strategy and conventional stiff position control strategy.

In Fig. 7(a), arithmetic average of 5 consecutive right foot GRF peaks are normalized via total weight and displayed both for VAC (purple) and conventional (green) methods. It may be observed that VAC method provides sufficient compliance while the exoskeleton is interacting with the environment, so that GRF levels are greatly reduced for about 65%. Therefore, comparing to the conventional method, VAC may provide exoskeleton-supported walking in a more physically-viable manner.

With the help of compliant walking support, a VAC-based controlled exoskeleton requires comparatively less upper body motion effort. Keeping this in mind, horizontal torso acceleration, torso pitch angle rate, and total force exerted by arms variations are displayed in Fig. 7(b)-(c)-(d) to defend this hypothesis. Examining these figures, such quantities show certain amount of decreases while VAC is applied. Table II sums up the complete results, in which percentage decreases are given in terms of RMS (Root Mean Square).

As previously discussed, the proposed VAC method automatically manages the position/force trade-off; within the presence of large force errors, it sacrifices joint tracking through a period, until the disturbance that introduced force error vanishes. Fig. 7(e) exhibits right leg knee joint tracking performances. Analyzing this figure, we obtained perfect joint tracking while the conventional method is used. VAC method also provides a feasible tracking performance, except touch-down instants which are indicated with blue circles. During those instants, joint tracking error follows a trend around 6 degrees. This appears to be the price to be paid for compliant walking support. On the other hand, this is a very affordable price; such tracking performance does not cause any problem during walking. In the multimedia attachment, we display both walking performances simultaneously, thus, one can confirm that possible motion differences between 2 walking experiments (with VAC and with conventional) are completely negligible [13].

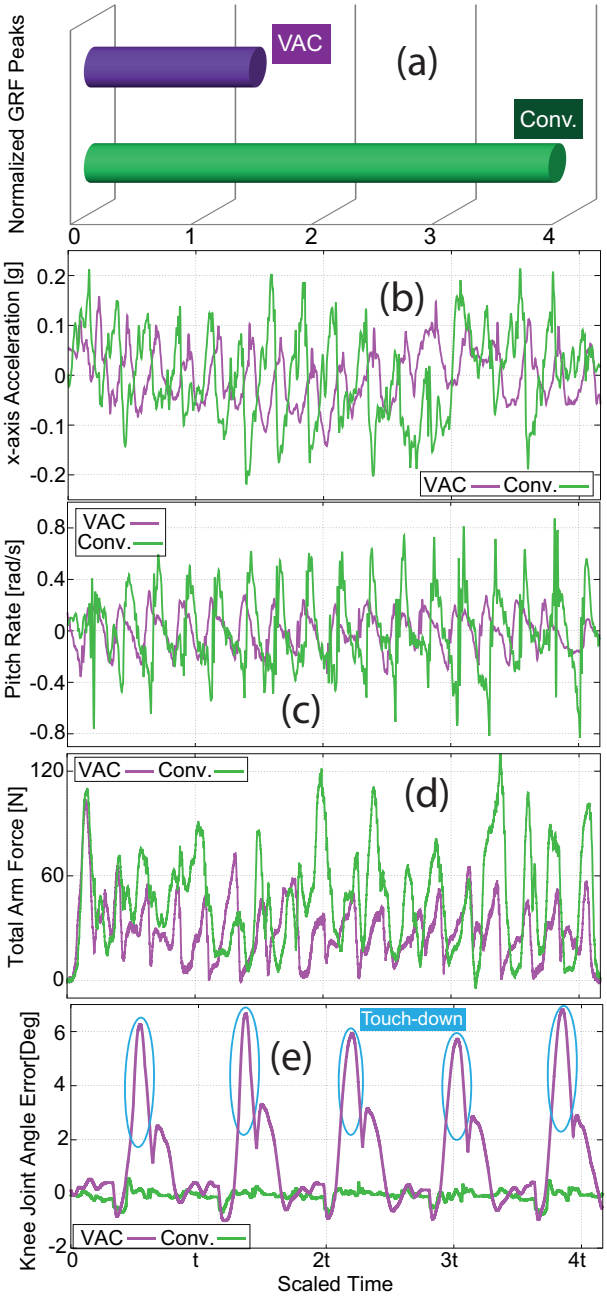

Fig. 7. Experiment #1 results, Subject #1.

B. *Experiment #2: Irregular Surface Walking*

Having concluded Experiment #1, we proceed to Experiment #2, in which hard wooden blocks with 3 [cm] heights are sequentially left on the treadmill. The human subject finds himself in an obligation to step on these blocks. Since this experiment is rather risky, only Subject #2 is asked to perform. Results are presented in Fig. 8, in which solid purple and green lines point out the data affiliated with VAC method and conventional method, respectively. Due to space limitation, only horizontal torso acceleration, torso pitch angle rate and total force exerted by arms are provided.

Scrutinizing Fig. 8, we can claim that VAC method is also

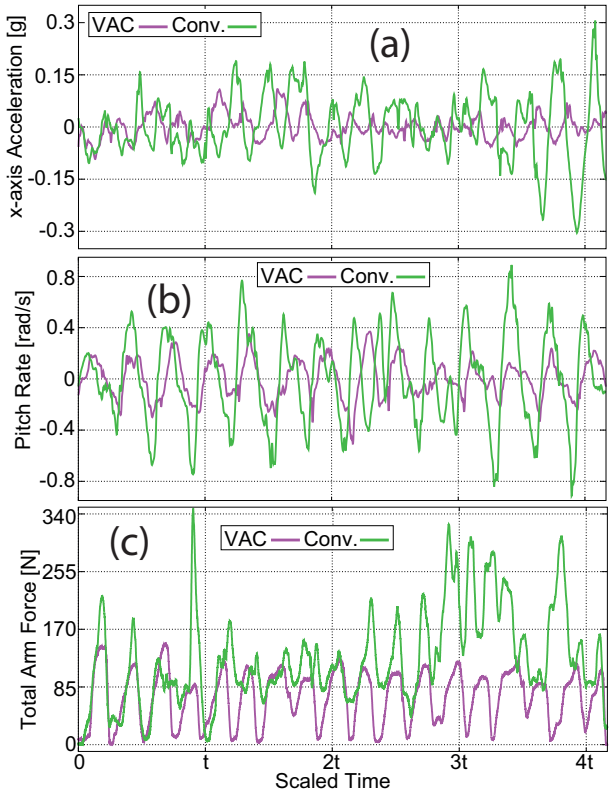

Fig. 8. Experiment #2 results, Subject #2.

efficient within the presence of irregularities on the surface. Comparing to conventional position control, we obtained %64 decrease in horizontal torso acceleration, %57 decrease in torso pitch angle rate, and %43 decrease in total force exerted by the subject's arms. Judging by these results, VAC method is able to provide physically viable walking support even the subject has to step on obstacles. While the exoskeleton is run on conventional method, the able-bodied subject experiences severe difficulties when he is stepping on wooden obstacles; he has to force himself in an utmost level to retrieve the overall dynamic balance.

VI. Conclusions and Future Directions

To conclude, we propose a motion generation method and a controller scheme, which are unified on an active lower body exoskeleton system for the robot-assisted paraplegia walking support task. It is shown that the motion generator is able to synthesize smooth, continuous and time-varying position references that are required for the task. The proposed controller, Virtual Admittance Controller, is also validated to be efficient, as it introduces virtual admittance in each joint to enhance environmental interaction capability. The controller simultaneously processes both position and force constraints while automatically managing the position/force trade-off.

Implementing the proposed method, exoskeleton-based bipedal walking support experiments are conducted with the help of 4 able-bodied human subjects. As the result, the controller is able to handle external forces in a more compliant and physically-viable manner, comparing to conventional stiff position control. Additionally, irregular surface walking experiments are conducted; an important case that is not heavily investigated in the literature. The results of this experiment also evaluated to be promising, indicating that VAC has potentials to be utilized for the paraplegia walking support task within the presence of obstacles on the surface.

In our future work, we conduct more experiments on numerous able-bodied subjects with different BMI levels, so as to cogently validate that the incorporation of compliance minimizes the upper body effort in the exoskeleton-supported walking task. Subsequently, clinical trials will be planned.

Acknowledgments

All the experiments are approved by the internal ethics review board. B. Ugurlu additionally acknowledges the support by MEXT/JSPS KAKENHI with Grant Number 23120004. The authors would like to thank S. T. Ahi, N. I. Ahi, S. Kojima, S. Miura, I. C. Ugurlu, K. Kotaka and J. Abdurrahim for their kind assistance.

References

[1] A. M. Dollar, and H. Herr, "Lower extremity exoskeletons and active orthoses: Challenges and state-of-the-art", in *IEEE Trans. on Robotics*, vol. 24, no. 1, 2008, pp. 144-158.

[2] T. Sumiya, K. Kawamura, A. Tokuhiro, H. Takechi, and H. Ogata, "A survey of wheelchair use by paraplegic individuals in Japan. Part2: Prevalence of pressure sores", in *Spinal Cord*, vol. 35, no. 9, 1997, pp. 595-598.

[3] H. Kazerooni, "Human augmentation and exoskeleton systems in Berkeley", in *Int. Journal of Humanoid Robotics*, vol. 4, no. 3, 2007, pp. 575-605.

[4] A. Esquenazi, M. Talaty, A. Packel, M. Saulino, "The ReWalk powered exoskeleton to restore ambulatory function to individuals with thoracic-level motor-complete spinal cord injury", in *American Journal of Phys. Med. Rehabil.*, vol. 91, no. 11, 2012, pp. 911-921.

[5] T. Kagawa, and Y. Uno, "Gait pattern generation for a power-assist device of paraplegic gait", in *Proc. IEEE Symp. on Robot and Human Interactive Communication*, Toyama, Japan, 2009, pp. 633-658.

[6] K. Suzuki, M. G. Kawamoto, H. Hasegawa, and Y. Sankai "Intention-based walking support for paraplegia patients with robot suit HAL", in *Advanced Robotics*, vol. 21, no. 12, 2007, pp. 1441-1469.

[7] D. G. Caldwell, N. G. Tsagarakis, S. Kousidou, N. Costa, and I. Sarakoglou, "'Soft' exoskeletons for upper and lower body rehabilitation - Design, control and testing", in *Int. Journal of Humanoid Robotics*, vol. 4, no. 3, 2007, pp. 549-573.

[8] J. F. Veneman, R. Kruidhof, E. E. G. Hekman, R. Ekkelenkamp, E. H. F. Van Asseldonk, and H. van der Kooij, "Design and evaluation of LOPES exoskeleton robot for interactive gait rehabilitation", in *IEEE Trans. on Neural Systems and Rehabilitation Engineering*, vol. 15, no. 3, 2007, pp. 379-386.

[9] P. D. Neuhaus, J. H. Noorden, T. J. Craig, T. Torres, J. Kirschbaum and J. E. Pratt, "Design and evaluation of Mina, a robotic orthosis for paraplegics", in *Proc. IEEE Conf. on Rehabilitation Robotics*, Zurich, Switzerland, 2011, pp. 1-8.

[10] B. Ugurlu, M. Nishimura, K. Hyodo, M. Kawanishi, and T. Narikiyo, "A framework for sensorless torque estimation and control in wearable exoskeletons", in *Proc. of the IEEE Worksh. on Advanced Motion Control*, Sarajevo, Bosnia&Herzegovina, 2012, pp. 1-7.

[11] N. Jarrasse, and G. Morel, "Connecting a human limb to an exoskeleton", in *IEEE Trans. on Robotics*, vol. 28, no. 3, 2012, pp. 697-709.

[12] B. Ugurlu, T. Kawasaki, M. Kawanishi, and T. Narikiyo, "Continuous and dynamically equilibrated one-legged running experiments: Motion generation and indirect force feedback control", in *Proc. IEEE Conf. on Intelligent Robots and Systems*, Algarve, Portugal, 2012, pp. 1846-1852.

[13] TTI Japan, Control Systems Laboratory YouTube Channel, "Ugurlu and Oshima, IEEE ICRA 2014, Exoskeleton-based Compliant Bipedal Walking Support" [Online]: http://youtu.be/2I9UkVpefJU